Received: 17 April 2018 | Revised: 22 August 2018 | Accepted: 10 October 2018

DOI: 10.1002/ccd.27953

WILEY

ORIGINAL STUDIES

Safety of catheter-based radiofrequency renal denervation on branch renal arteries in a porcine model

Atsushi Sakaoka PhD[1] | Serge D. Rousselle DVM[2] | Hitomi Hagiwara BS[1] | Armando Tellez MD[2,3] | Brad Hubbard DVM[4] | Kenichi Sakakura MD[5]

[1]Evaluation Center, R&D Administration and Promotion Department, Terumo Corporation, Kanagawa, Japan

[2]Alizée Pathology, LLC, Thurmont, Maryland

[3]Tecnologico de Monterrey, Escuela de Medicina y Ciencias de la Salud, Monterrey, Mexico

[4]Synchrony Labs, LLC, Durham, North Carolina

[5]Division of Cardiovascular Medicine, Saitama Medical Center, Jichi Medical University, Saitama, Japan

Correspondence
Atsushi Sakaoka, PhD, Evaluation Center, R&D Administration and Promotion Department, Terumo Corporation, 1500 Inokuchi, Nakai-machi, Ashigarakami-gun, Kanagawa 259-0151, Japan.
Email: atsushi_sakaoka@terumo.co.jp

Funding information
Terumo Corporation, Tokyo, Japan

Abstract

Objectives: We aimed to investigate the safety of radiofrequency (RF)-renal denervation (RDN) on branch renal arteries (RAs) in a porcine model.

Background: The efficacy of RF-RDN was enhanced by treatment of the branch RA, in addition to the main RA. However, there are concerns regarding the safety of RF-RDN on branch RA because of their smaller diameter and proximity to the kidney.

Methods: RF was delivered to 24 RA from 12 swine. A total of 8 RA from 4 swine were untreated. Treated RA were examined by angiography and histopathology at 7, 30, and 90 days. Serum creatinine concentration, biophysical parameters during RF delivery, and renal norepinephrine concentration were also assessed.

Results: Angiography revealed minimal late lumen loss and diameter stenosis in the main and branch RA at any time point. There was no change in serum creatinine after RF-RDN. Histopathologically, no augmentation of medial damage or neointimal formation was found in branch RA compared with main RA. No or minimal damage to surrounding tissues including the kidneys, ureters, lymph nodes, and muscles was observed at any time point in both the main and branch RA. Equivalent electrode temperature in the main and branch RA was achieved by automatic adjustment of output power by the generator. The renal norepinephrine concentration was significantly lower in the treated group compared with the untreated group.

Conclusions: RF-RDN on branch RA was safe in a porcine model, with stenosis-free healing of treated arteries and negligible kidney damage at 7, 30, and 90 days.

KEYWORDS

branch renal artery, pathology, preclinical study, radiofrequency, renal denervation

1 | INTRODUCTION

Catheter-base renal denervation (RDN) with radiofrequency (RF) has been used recently as an anti-hypertensive treatment option.[1] Since RDN failed to meet a primary efficacy endpoint of lowering blood pressure in the SYMPLICITY HTN-3 trial,[2] clinical interest in RDN has predominantly focused on enhancing efficacy rather than confirming safety.[1,3,4] Importantly, a recent anatomical study showed that the renal sympathetic nerve fibers are distributed closer to the lumen in branch renal arteries (RAs) compared with the main RA,[5] suggesting that RDN that includes the branch RA may ablate more sympathetic nerves than RDN on the main RA alone.[6] This hypothesis was supported in recent animal and clinical studies including the blinded, randomized, sham-controlled SPYRAL HTN-OFF MED and ON MED trials.[7–14] Direct comparison studies in animals and humans clearly confirmed greater efficacy in RDN on both branch and main RA compared with RDN on main RA alone.[7–10] Therefore, branch RA is expected to become the treatment site of choice for RF-based RDN.

The safety of RF-RDN on the main RA has been confirmed in >1,000 patients,[2,15–18] and histopathological changes induced by RF-RDN around the main RA were assessed in several animal studies,[7,19–24] However, the safety of RF-RDN on the branch RA

remains unclear. As the diameter of the branch RA is smaller than that of the main RA, there is a potential risk of disruption or stenosis. Moreover, as branch RA are located adjacent to the kidney, there is a risk of renal damage and impairment of renal function. As prior animal studies of branch RF-RDN were largely focused on its efficacy, the safety of RF-RDN on the branch RA has not been fully investigated.[7,11] Thus, the aim of the present study was to investigate the safety of RF-RDN on branch RA in a porcine model at 7, 30, and 90 days.

2 | METHODS

2.1 | RDN system

The IberisBloom RDN system (Terumo Corporation, Tokyo, Japan) used in the present study consists of a helical multi-electrode catheter and a multi-channel generator, as previously described.[25] The generator delivers RF (with 6 W for 60 sec) to selected electrodes simultaneously. The IberisBloom system has an automatic algorithm that decreases output power by 1 W in the channel when the corresponding electrode temperature is ≥70°C for 1 sec.

2.2 | Animals

All animal procedures were approved by the Institutional Animal Care and Use Committee before study conduct. Table 1 summarizes the study design. A total of 16 female Yorkshire crossbred swine (55.8–68.4 kg) were randomly allocated to four groups: an untreated group, and RF treated groups with 7-, 30-, and 90-day time points. All animals received aspirin (325 mg/os) daily from day 0 until the scheduled necropsy. Blood was collected at day 0 and the terminal day to measure serum creatinine concentration. RAs of 12 animals were treated bilaterally with the IberisBloom system at day 0. Anticoagulation during the catheterization was achieved with intravenous heparin to maintain the activated clotting time at ≥250 sec. A 7F introducer sheath was placed by percutaneous cannulation of the femoral artery, and a 6F guide catheter was advanced to approach the RAs. Intra-arterial nitroglycerin (200 μg) was administered before angiography. Following quantitative vessel analysis (QVA), branch and main RA with diameters of 3–8 mm were treated. Treatment in the branch RA was limited to the outside of the renal parenchyma (hilum) as observed on fluoroscopy, following the protocol from recent clinical studies including branch RA treatment.[4,8]

TABLE 1 Assessment parameters in each group

Group Time point	Untreated group	Treated group		
		7 days	30 days	90 days
No. of animals (no. of arteries)	4 (8)	4 (8)	4 (8)	4 (8)
0 day				
Angiography (QVA)		X	X	X
Biophysical parameters during ablation		X	X	X
Serum creatinine	X	X	X	X
Follow-up day				
Angiography (QVA)		X	X	X
Renal tissue norepinephrine	X	X	X	X
Serum creatinine	X	X	X	X
Gross pathology and histopathology		X	X	X

Abbreviation: QVA, quantitative vessel analysis.
X indicates collection of data in the group.

At termination, treated animals underwent follow-up renal angiography after nitroglycerin administration (200 μg intra-arterial). A midline laparotomy was performed under general anesthesia in all animals to gain access to the kidneys. Samples of renal cortical tissues were removed from six sites (cranial, middle, and caudal area of the dorsal and ventral aspects of the kidney) per kidney for bioanalysis of norepinephrine concentration. A gross necropsy was performed on animals immediately following euthanasia. After perfusion fixation, RAs with surrounding tissues were harvested *en bloc* and immersed in 10% neutral-buffered formalin.

2.3 | Histopathology

Histological sections were produced at 3- to 5-mm intervals of the treated RA with surrounding tissues, as previously described,[26] and stained with hematoxylin–eosin and elastica Masson's trichrome. Endothelialization of the RA was circumferentially evaluated: 0 = endothelial coverage <25% of vessel circumference, 1 = endothelial coverage 25–50% of vessel circumference, 2 = endothelial coverage 51–75% of vessel circumference, 3 = endothelial coverage 76–95% of vessel circumference, and 4 = endothelial coverage >95% of vessel circumference. Inflammation was evaluated: 0 = no inflammation to minimal interspersed inflammatory cells anywhere in the relevant vessel compartment, 1 = mild peripheral inflammatory infiltration or focally moderate in <25% of the relevant vessel compartment, 2 = moderate peripheral inflammatory infiltration or focally marked in 25–50% of the relevant vessel compartment, and 3 = heavy peripheral inflammatory infiltration or focally marked in >50% of the relevant vessel compartment. Media thinning was evaluated: 0 = normal, 1 = minimal thinning of the media compared with adjacent intact levels (media thickness > 50% of normal), 2 = more pronounced segmental thinning of the media (media thickness < 50% of normal thickness with no tearing or laceration), and 3 = widespread marked thinning of the media (<25% of normal thickness). Media hyalinization/hypocellularity and fibrosis were circumferentially evaluated: 0 = not present, 1 = minimal (<1/3 of vessel circumference), 2 = mild (>1/3 and < 2/3 of vessel circumference), and 3 = moderate (>2/3 of vessel circumference). Any histopathological changes in surrounding tissues were evaluated: 0 = no change, 1 = present, but minimal feature, 2 = notable feature not effacing pre-existing tissue elements or limited to a small tissue area, and 3 = overwhelming feature involving large tissue areas. Lesion depth was measured with an ocular micrometer from the arterial lumen to that of the deepest damage.

2.4 | Biophysical parameters

The generator automatically measured biophysical parameters (output power, impedance, and electrode temperature) in real time during delivery of RF, as previously described.[25] Relative impedance

reduction (%) was calculated as 100 × (baseline impedance − terminal impedance) / baseline impedance. These parameters were documented per ablation. To analyze differences in the biophysical parameters between the main and branch RA, the located segment of each ablation was classified into main or branch RA based on angiographic appearance of the corresponding electrodes position. Among a total of 187 ablations, 14 ablations were excluded from the analysis as the corresponding electrodes may have been located in a bifurcation, and thus may have not been apposed well to the arterial wall.

2.5 | Renal norepinephrine concentration

Renal cortical tissue samples were immediately frozen by liquid nitrogen and stored at −80°C until bioanalysis. The tissue was homogenized, and the homogenate then analyzed by liquid chromatography with tandem mass spectrometry. Concentrations from each of the six sites from each kidney were then used to calculate the average per kidney.

2.6 | Statistical analysis

Data are presented as mean ± standard deviation. QVA and histopathological data were compared by unpaired *t* test between the main and branch RA. Renal norepinephrine concentration for each treated group was compared with those from the untreated group using the Dunnet test. A one-way analysis of variance (ANOVA) was used to examine differences in serum creatinine change from baseline to terminal across the groups. All statistical analyses were performed with statistical software (GraphPad Prism 7; GraphPad Software, San Diego, CA, USA). A *P*-value <0.05 was considered to indicate statistical significance.

3 | RESULTS

3.1 | In-life observations, serum chemistry, and necropsy

All animals survived until scheduled necropsy without any abnormalities caused by the RDN, as determined by daily clinical observation. There were no significant differences in serum creatinine change from baseline to terminal between the groups (0.0 ± 0.1 mg/dL in the untreated group, 0.0 ± 0.2, 0.3 ± 0.2, and 0.2 ± 0.3 mg/dL at 7, 30, and 90 days, respectively, in the treated groups; $P = 0.15$ for all). For gross necropsy, all tissues were normal with the exception of one incidental renal cyst, which is a common spontaneous lesion observed in swine (incidence 6.3%).[27]

3.2 | Procedural and angiographic outcomes

The mean baseline lumen diameter of the branch RA was significantly smaller than those of the main RA (Figure 1). The number of ablations per animal was 14.8 ± 2.6 in the 7-day group, 14.5 ± 2.4 in the 30-day group, and 17.5 ± 4.8 in the 90-day group. While luminal irregularities known as "notches" were frequently observed just after treatment, no angiographic abnormalities were observed in the main or branch RA at 7, 30, and 90 days after treatment (Figure 2). QVA indicated that the late lumen loss and diameter stenosis were minimal in the main and branch RA at 7, 30, and 90 days (Figure 1).

3.3 | Histopathology

Treated arterial lumens were almost completely covered by endothelial cells at 7 days, and completely covered at 30 and 90 days, in both the main and branch RA (Table 2, Figure 3). The treated media was hyalinized and thinned with smooth muscle cell loss at 7 days, while treated media showed fibrosis instead of hyalinization and thinning at 30 and 90 days (Table 2, Figure 3). Neointima, which formed over the

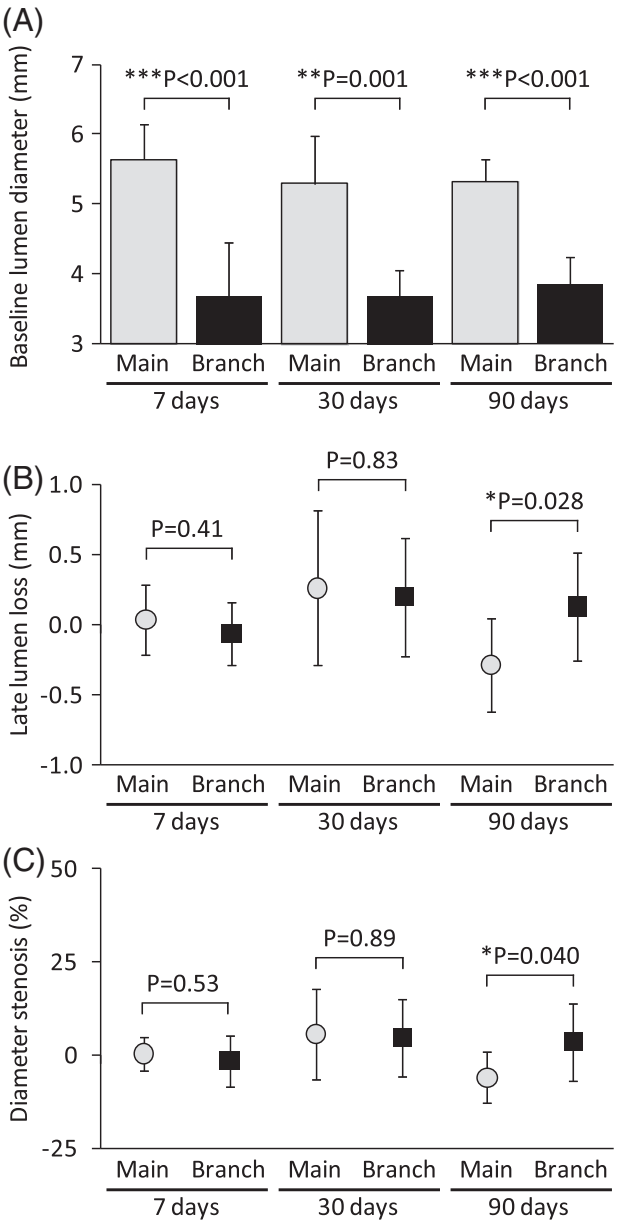

FIGURE 1 Baseline lumen diameter (A) of the main and branch RAs in each group. Late lumen loss (B) and percent diameter stenosis (C) based on follow-up QVA at each time point. Baseline lumen diameter of the main RA was larger than that of the branch RA at all-time points. Late lumen loss and diameter stenosis were overall minimal at all-time points. Although there were statistically significant differences between the main and branch RA at 90 days, they were minimal and of minor clinical significance

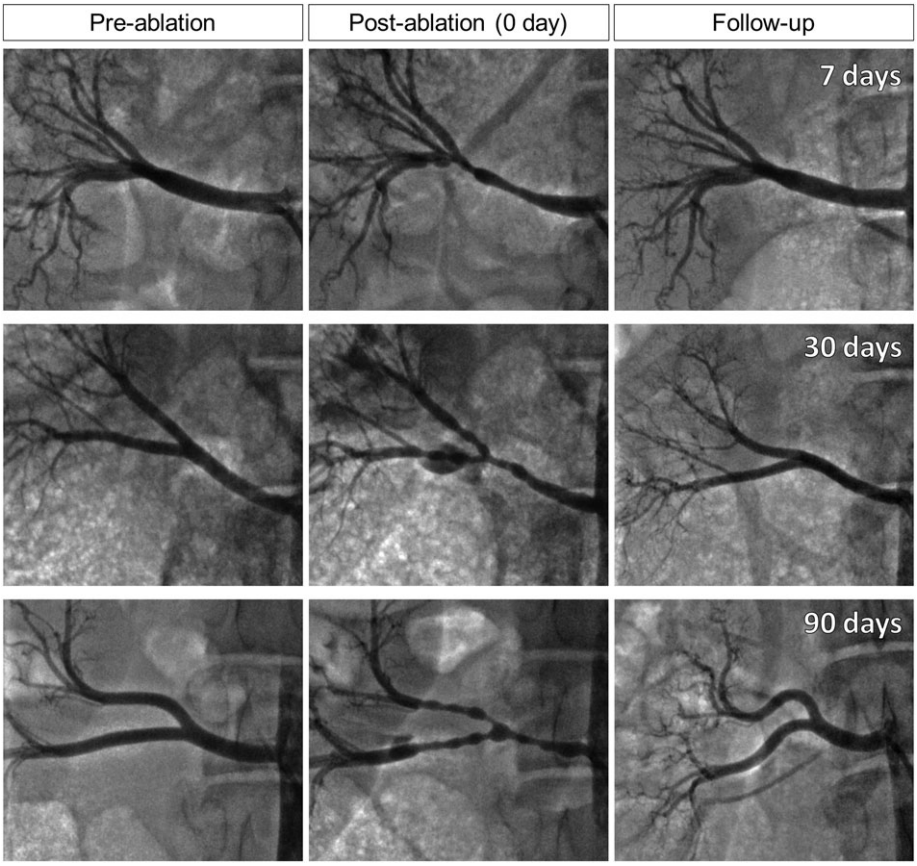

FIGURE 2 Representative angiographic images of treated RA at pre-ablation, post-ablation, and follow-up (7, 30, and 90 days). Immediately after RF ablation, multiple notches led to luminal irregularity, while no other abnormalities such as dissection or perforation were found. Follow-up angiography indicated disappearance of the luminal irregularity and no stenotic signs

healed treated media, was minimal at all time points (Figure 3). Medial damage and minimal neointimal formation were common to the main and branch RA, and no augmentation was found in the branch RA compared with the main RA. Damage in surrounding tissues including the kidneys, ureters, lymph nodes, and muscles were none or minimal at all time points in both the main and branch RA, while mild necrosis/inflammation was noted in adipose tissues at 7 days (Table 2). At 7 days, minimal focal necrosis was observed in the edge of the kidney adjacent to a treated branch RA in one of eight kidneys (Figure 4A), although the damaged area was small (approximately 1.7 × 0.8 mm). No kidney necrosis was found at 30 and 90 days. At 90 days, a remnant of earlier kidney damage was identified as minimal and focal fibrosis in the edge of one of eight kidneys (approximately 1.5 × 0.3 mm, Figure 4B). The renal parenchyma (renal tubules and glomeruli) was normal beneath the fibrosis area.

3.4 | Biophysical parameters

The biophysical parameters are summarized in Table 3. Terminal output power in the branch RA (3.7 W) was significantly lower than that in the main RA (4.4 W), indicating that an automatic decrease in the output power from 6.0 W (set value) was activated more frequently in the branch RA than in the main RA. However, terminal electrode temperature was equivalent in the main RA (64.2°C) and the branch RA (66.2°C). Baseline impedance, terminal impedance, and impedance reduction during ablation were higher in the branch RA than in the main RA.

3.5 | Renal norepinephrine concentration

Compared with the renal norepinephrine concentration in the untreated group (204.1 ± 38.7 ng/g), renal norepinephrine concentration in the treated groups was significantly reduced to 49.5 ± 37.5 ng/g at 7 days ($P < 0.001$), 50.4 ± 33.1 ng/g at 30 days ($P < 0.001$), and 121.5 ± 61.2 ng/g at 90 days ($P = 0.002$).

4 | DISCUSSION

We demonstrated that RF-RDN on branch RA was safe by comparing angiographic and histopathological parameters between the main and branch RA from 7 days (subacute time point) to 90 days (chronic time point) in a porcine model. Despite the smaller diameters of the branch RA and the anatomical proximity of the branch RA to the kidney, there was no evidence of stenosis, and only negligible kidney damage, at any time point following branch treatment, as confirmed by angiography, histopathology, and serum creatinine measurement. Recent clinical trials showed a significant blood pressure-lowering effect of RDN on branch RA.[8,9,12,13] However, the long-term safety of branch treatment has not been fully examined in clinical trials. To predict the risk of branch treatment in the clinical setting, we followed the clinical

TABLE 2 Histopathological data in main and branch RA at each time point

Time point	7 days			30 days			90 days		
Segment	Main	Branch	*P* value	Main	Branch	*P* value	Main	Branch	*P* value
RA									
Endothelialization (score 0–4)	3.93 ± 0.10	4.00 ± 0.00	0.08	4.00 ± 0.00	4.00 ± 0.00	…	4.00 ± 0.00	4.00 ± 0.00	…
Inflammation (score 0–3)	0.00 ± 0.00	0.00 ± 0.00	…	0.00 ± 0.00	0.00 ± 0.00	…	0.00 ± 0.00	0.00 ± 0.00	…
Media thinning (score 0–3)	0.53 ± 0.27	0.13 ± 0.15	**0.003**	0.10 ± 0.19	0.00 ± 0.00	0.15	0.00 ± 0.00	0.00 ± 0.00	…
Media hyalinization/ hypocellularity (score 0–3)	0.55 ± 0.17	0.17 ± 0.23	**0.003**	0.18 ± 0.19	0.03 ± 0.07	**0.050**	0.00 ± 0.00	0.00 ± 0.00	…
Media fibrosis (score 0–3)	0.06 ± 0.12	0.00 ± 0.00	0.15	0.91 ± 0.35	0.13 ± 0.16	**<0.001**	0.87 ± 0.28	0.20 ± 0.10	**<0.001**
Surrounding tissues (score 0–3)									
Adipose tissue necrosis/ inflammation	0.70 ± 0.21	0.19 ± 0.17	**0.001**	0.06 ± 0.08	0.00 ± 0.00	0.07	0.00 ± 0.00	0.00 ± 0.00	…
Kidney necrosis	0.00 ± 0.00	0.03 ± 0.07	0.33	0.00 ± 0.00	0.00 ± 0.00	…	0.00 ± 0.00	0.00 ± 0.00	…
Ureter necrosis	0.00 ± 0.00	0.00 ± 0.00	…	0.00 ± 0.00	0.00 ± 0.00	…	0.00 ± 0.00	0.00 ± 0.00	…
Lymph node necrosis	0.00 ± 0.00	0.00 ± 0.00	…	0.00 ± 0.00	0.00 ± 0.00	…	0.00 ± 0.00	0.00 ± 0.00	…
Muscle necrosis	0.06 ± 0.12	0.02 ± 0.05	0.33	0.00 ± 0.00	0.00 ± 0.00	…	0.00 ± 0.00	0.00 ± 0.00	…
Lesion depth (mm)	3.78 ± 1.75	2.98 ± 1.23	0.39	3.15 ± 1.36	1.80 ± 0.60	0.09	2.09 ± 0.94	1.58 ± 0.51	0.20

Data are presented as mean ± standard deviation. *P* values were calculated with an unpaired *t* test.

procedural protocol whereby treatment is limited to arterial segments outside of the renal parenchyma.[4,8]

4.1 | Effects of branch treatment on RAs

Histopathological changes after RF-RDN on the main RA were previously reported in porcine models.[20–22,28] In support of previous data,[22] we found that endothelial cells covered the treated luminal surface almost completely at 7 days in both the main and branch RA. Sakakura et al. reported that medial thinning and hypocellularity (loss of smooth muscle cells) in the main RA were most evident at 7 days, and then resolved at later time points (30, 60, and 180 days).[22] Rippy et al.[28] also described healing of medial damage (evident as fibrosis) at 6 months after RF-RDN on the main RA. In this study, the chronological transition of RF-induced medial damage in both the main and branch RA was consistent with that reported in earlier porcine studies in the main RA. The study by Rippy et al. also reported minimal neointimal thickening composed of several cell layers at 6 months after RF-RDN.[28] Similarly, in the present study the neointimal thickness was minimal (several cell layers at most) in the both main and branch RA at all time points, and there was no evidence of stenosis at any level. Our QVA results also showed minimal late lumen loss and percent diameter stenosis in both the main and branch RA at all time points. Therefore, branch treatment would be unlikely to increase the risk of stenosis compared with treatment on main RA in the clinical settings. Nevertheless, we should note that new occurrence of severe stenosis has been clinically reported after RF-RDN on main RA,[29–31] while the occurrence rate was considerably low in large-scale studies (0 of 364 and 1 of 998 patients at 6 months after treatment in the SYMPLICITY HTN-3 trial[32] and the Global SYMPLICITY registry[15] respectively).

4.2 | Effects of branch treatment on the kidney and surrounding tissues

Branch treatment caused necrosis in one of eight kidneys at 7 days, although the damaged area was small and limited to the focal edge of the kidney. At 90 days, a focal damaged area was found at the edge of the kidney and identified by fibrosis, a sign of healing, in one of eight kidneys. No elevation of serum creatinine was observed in any treated groups, indicating that renal function was unaffected. Therefore, occasional kidney damage by branch treatment may be negligible, as long as RF treatments are limited to the outside of the kidney under fluoroscopy. Adipose tissue necrosis/inflammation, which was previously reported in RF-RDN on the main RA,[20] was mainly found at 7 days in the present study. This change was not augmented in the branch RA compared with the main RA, suggesting no increased risk of branch treatment. Lesion depth was greatest at 7 days, and then reduced at later time points (because of healing) in both the main and branch RA, similar to that previously reported in RF-RDN on the main RA.[22] Lesion depth was also lower in the branch RA than that in main RA at all time points. Although the underlying mechanism remains unclear, this finding is consistent with a previous porcine study using another RF-delivering device, the Symplicity Spyral.[19]

4.3 | Biophysical parameters

Electrode temperature is determined by the balance of heat gain diffusing from tissues and heat loss by blood flow.[33] Blood flow in the branch RA is less than that in the main RA because of the smaller

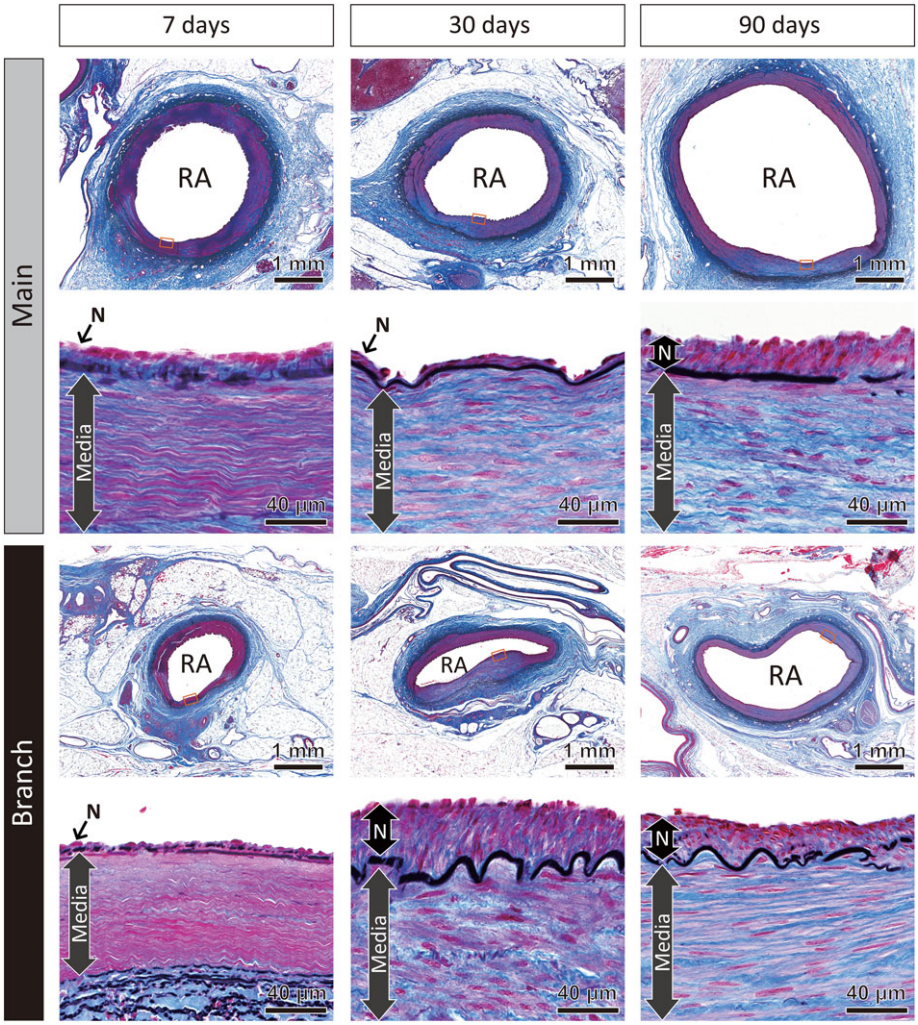

FIGURE 3 Representative histopathological images of the treated main and branch RA at 7, 30, and 90 days. The images in the second- and fourth-row panels are magnified images of the boxed area in the first- and third-row panels, respectively. At 7 days, treated media was hyalinized (red-stained without smooth muscle cells) and thinned. At 30 and 90 days, treated media showed fibrosis (blue-stained fibers between cells). Thickness of the neointima (indicated as "N"), which was formed on the internal elastic lamina (dark-purple-stained fiber), was minimal at all time points. These histopathological changes were common to both the main and branch RA. Elastica Masson's trichrome staining. Scale bars: 1 mm (the first- and third-row panels; 40 μm (the second- and fourth-row panels) [Color figure can be viewed at wileyonlinelibrary.com]

vessel diameter, resulting in a more rapid elevation of electrode temperature in the branch RA during RF delivery. Thus, branch treatment has the potential to produce excessive heating and subsequent unfavorable arterial damage. However, the present study showed that electrode temperature in the branch RA (66.2°C) was equivalent to that in main RA (64.2°C), and there was no increase in histopathological arterial damage in the branch RA. The equivalent electrode temperature was likely a result of the automatic control mechanism of the IberisBloom system, which decreases output power when electrode temperature reaches ≥70°C, as shown by the significantly lower terminal output power in the branch RA compared with the main RA.[25] However, impedance was higher when the electrode was located in the branch RA than in the main RA. Generally, a higher impedance relates to an increased contact force of an electrode to local tissues.[34,35] The IberisBloom catheter has a self-expanding design, which allows the electrodes to be well apposed on the arterial wall in smaller-diameter vessels, resulting in higher impedance in the branch RA. Therefore, the IberisBloom system maintained a sufficient electrode temperature to induce protein denaturation in tissues, but without excessive heating.

4.4 | Renal norepinephrine concentration

Denervation was successfully achieved in the present study, as shown by a significant reduction of renal norepinephrine concentration in the treated groups compared with the untreated group. However, the reduction of renal norepinephrine concentration was less at 90 days than at 7 and 30 days. This result is in line with previous studies using healthy swine.[24,36] Although the recovery mechanism has not yet been elucidated, previous animal studies suggest contribution of nerve regeneration.[26,37] Considering the long-lasting effects of RDN in humans,[38] recovery of renal norepinephrine concentration as early as 3 months after RDN seems to be specific to healthy animals.

4.5 | Procedural consistency with recent clinical trials

The average number of ablations per patient varied from 14 to 45.9 among clinical studies which investigated the effect of branch

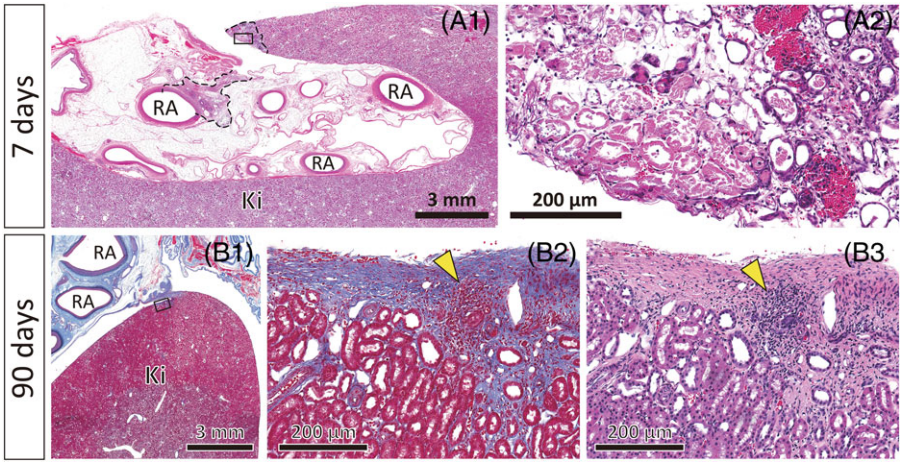

FIGURE 4 A, The most severe kidney damage at 7 days. Panel A2 is a magnified image of the boxed area in panel A1. Dotted line in panel A1 indicates a borderline of ablated area. There was only a focal area of damage on the edge of the kidney parenchyma, with necrosis of the renal tubules, hemorrhage, infiltration of mononuclear cells, and mineralization. B, Remnant of kidney damage at 90 days. Panel B2 and B3 are magnified images of the boxed area in B1. The focal edge of the kidney showed fibrosis (blue-stained area in panel B2) and infiltration of mononuclear cells (arrowheads in panel B2 and B3). RA indicates lumen of the RA; Ki, kidney. Hematoxylin and eosin staining (A1, A2, B3) and elastica Masson's trichrome staining (B1, B2). Scale: 3 mm (A1, B1); 200 μm (A2, B2, B3) [Color figure can be viewed at wileyonlinelibrary.com]

treatment.[8,10,12–14] Even considering the variation in clinical studies, the number of ablations seems to be smaller in the present study (14.5–17.5) compared with the clinical studies. The possible reason for the discrepancy is an anatomical difference between swine and human. The main RA is shorter in swine compared with human,[39] resulting in a smaller number of ablations in swine. Since, to date, length or diameter of human branch RA have not been systemically investigated, it is still unknown if branch RAs are also anatomically different between swine and human. Such anatomical difference may affect the number of ablations.

Despite the difference in the number of ablations, we followed the same procedural protocol as in SPYRAL HTN-OFF MED and ON MED trials in how distal segment are treated; the treatment was limited to arteries of 3-8 mm in diameter and to the outside of the renal parenchyma as observed on fluoroscopy.[4] This procedural consistency suggests that the most distal branch arterial segment, where the potential risk for stenosis of small-diameter RA and damages in kidney parenchyma is the highest, were treated in the same manner as in the above clinical trials. Therefore, the present study appropriately assessed safety of branch RF-RDN.

TABLE 3 Biophysical parameters of ablation in main and branch RA

	Main	Branch	*P* value
Number of ablations	119	54	
Output power at ablation termination (watt)	4.4 ± 1.2	3.7 ± 1.3	**0.0005**
Terminal electrode temperature (°C)	64.2 ± 6.8	66.2 ± 7.9	0.09
Baseline impedance (Ω)	202 ± 15	216 ± 18	**<0.0001**
Terminal impedance (Ω)	182 ± 13	191 ± 14	**<0.0001**
Impedance reduction during ablation (%)	10.0 ± 2.9	11.2 ± 4.3	**0.0285**

Data are presented as mean ± SD. *P* values were calculated with an unpaired *t* test.
Bold text indicates statistical significance (P<0.05).

4.6 | Significance of branch treatment

Several different technologies are used in current RDN devices: RF, ultrasound,[40,41] and alcohol injection.[42] The second-generation RF-RDN devices (Symplicity Spyral and IberisBloom) allow RF to be applied in branch RA. Meanwhile, current ultrasound- and alcohol-RDN devices are designed for main RA alone. Due to a paucity of direct comparison among different technologies/devices, it is currently uncertain which device/technology is clinically most beneficial. However, considering that patients with short main RA (i.e., early bifurcation) would not be suitable for RDN devices designed exclusively for main RA, it would be meaningful to investigate safety and efficacy of branch treatment with RF-RDN devices.

4.7 | Study limitations

The present study has some limitations. First, the findings obtained from the normotensive swine may not be applicable to patients with hypertension. However, the normotensive swine is the standard animal model for assessing RDN device safety, because of its anatomical and physiological similarity to humans.[7,19,21–23,25,26,28] Second, because of the small number of animals, adverse findings with a low incidence may have been missed. Further, although the safety profile was comparable between the branch RA and main RA, there is an inherent risk of beta error with a small sample size. Third, the RDN device in the present study was applied in branch RA following the manufacturer's instruction, and thus the study result may not be transferrable to other RDN devices which are not indicated for branch RA.

5 | CONCLUSIONS

RF-RDN on the branch RA was safe in a porcine model, as shown by no stenotic signs and negligible kidney damage at 7, 30, and 90 days.

ACKNOWLEDGMENTS

We thank Edanz Group for editing a draft of this manuscript.

CONFLICT OF INTEREST

Dr Sakaoka and Ms Hagiwara are employees of Terumo Corporation. Dr Sakakura has received speaking honoraria from Abbott Vascular, Boston Scientific, Medtronic Cardiovascular, Terumo, OrbusNeich, and NIPRO. He has also served as a consultant for Abbott Vascular and Boston Scientific.

ORCID

Atsushi Sakaoka https://orcid.org/0000-0002-3656-8277
Kenichi Sakakura https://orcid.org/0000-0003-3566-0394

REFERENCES

1. Mahfoud F, Schmieder RE, Azizi M, et al. Proceedings from the 2nd European clinical consensus conference for device-based therapies for hypertension: state of the art and considerations for the future. Eur Heart J. 2017;38(44):3272-3281.
2. Bhatt DL, Kandzari DE, O'Neill WW, et al. A controlled trial of renal denervation for resistant hypertension. N Engl J Med. 2014;370(15):1393-1401.
3. Kandzari DE, Bhatt DL, Brar S, et al. Predictors of blood pressure response in the SYMPLICITY HTN-3 trial. Eur Heart J. 2015;36(4):219-227.
4. Kandzari DE, Kario K, Mahfoud F, et al. The SPYRAL HTN global clinical trial program: rationale and design for studies of renal denervation in the absence (SPYRAL HTN OFF-MED) and presence (SPYRAL HTN ON-MED) of antihypertensive medications. Am Heart J. 2016;171(1):82-91.
5. Sakakura K, Ladich E, Cheng Q, et al. Anatomic assessment of sympathetic peri-arterial renal nerves in man. J Am Coll Cardiol. 2014;64(7):635-643.
6. Mahfoud F, Edelman ER, Bohm M. Catheter-based renal denervation is no simple matter: Lessons to be learned from our anatomy? J Am Coll Cardiol. 2014;64(7):644-646.
7. Mahfoud F, Tunev S, Ewen S, et al. Impact of lesion placement on efficacy and safety of catheter-based radiofrequency renal denervation. J Am Coll Cardiol. 2015;66(16):1766-1775.
8. Fengler K, Ewen S, Hollriegel R, et al. Blood pressure response to Main renal artery and combined Main renal artery plus branch renal denervation in patients with resistant hypertension. J Am Heart Assoc. 2017;6(8):e006196.
9. Pekarskiy SE, Baev AE, Mordovin VF, et al. Denervation of the distal renal arterial branches vs. conventional main renal artery treatment: a randomized controlled trial for treatment of resistant hypertension. J Hypertens. 2017;35(2):369-375.
10. Petrov I, Tasheva I, Garvanski I, Stankov Z, Simova I. Comparison of standard renal denervation procedure versus novel distal and branch vessel ablation with brachial arterial access. Cardiovasc Revasc Med. 2018:S1553-8389(18)30213-6.
11. Henegar JR, Zhang Y, De Rama R, Hata C, Hall ME, Hall JE. Catheter-based radiorefrequency renal denervation lowers blood pressure in obese hypertensive dogs. Am J Hypertens. 2014;27(10):1285-1292.
12. Beeftink MM, Spiering W, De Jong MR, et al. Renal denervation beyond the bifurcation: the effect of distal ablation placement on safety and blood pressure. J Clin Hypertens (Greenwich). 2017;19(4):371-378.
13. Townsend RR, Mahfoud F, Kandzari DE, et al. Catheter-based renal denervation in patients with uncontrolled hypertension in the absence of antihypertensive medications (SPYRAL HTN-OFF MED): a randomised, sham-controlled, proof-of-concept trial. Lancet. 2017;390(10108):2160-2170.
14. Kandzari DE, Bohm M, Mahfoud F, et al. Effect of renal denervation on blood pressure in the presence of antihypertensive drugs: 6-month efficacy and safety results from the SPYRAL HTN-ON MED proof-of-concept randomised trial. Lancet. 2018;391(10137):2346-2355.
15. Bohm M, Mahfoud F, Ukena C, et al. First report of the global SYMPLICITY registry on the effect of renal artery denervation in patients with uncontrolled hypertension. Hypertension. 2015;65(4):766-774.
16. Esler MD, Krum H, Sobotka PA, Schlaich MP, Schmieder RE, Bohm M. Renal sympathetic denervation in patients with treatment-resistant hypertension (the Symplicity HTN-2 trial): a randomised controlled trial. Lancet. 2010;376(9756):1903-1909.
17. Kario K, Ogawa H, Okumura K, et al. SYMPLICITY HTN-Japan - first randomized controlled trial of catheter-based renal denervation in Asian patients. Circ J. 2015;79(6):1222-1229.
18. Worthley SG, Wilkins GT, Webster MW, et al. Safety and performance of the second generation EnligHTN renal denervation system in patients with drug-resistant, uncontrolled hypertension. Atherosclerosis. 2017;262:94-100.
19. Mahfoud F, Pipenhagen CA, Boyce Moon L, et al. Comparison of branch and distally focused main renal artery denervation using two different radio-frequency systems in a porcine model. Int J Cardiol. 2017;241:373-378.
20. Sakakura K, Ladich E, Edelman ER, et al. Methodological standardization for the pre-clinical evaluation of renal sympathetic denervation. JACC Cardiovasc Interv. 2014;7(10):1184-1193.
21. Sakakura K, Ladich E, Fuimaono K, et al. Comparison of renal artery, soft tissue, and nerve damage after irrigated versus nonirrigated radiofrequency ablation. Circ Cardiovasc Interv. 2015;8(1):e001720.
22. Sakakura K, Tunev S, Yahagi K, et al. Comparison of histopathologic analysis following renal sympathetic denervation over multiple time points. Circ Cardiovasc Interv. 2015;8(2):e001813.
23. Sakaoka A, Takami A, Onimura Y, et al. Acute changes in histopathology and intravascular imaging after catheter-based renal denervation in a porcine model. Catheter Cardiovasc Interv. 2017;90(4):631-638.
24. Hubbard B, Sakaoka A, Brants IK, et al. Sub-acute safety and efficacy evaluation of a single versus double treatment cycles of a monopolar radiofrequency catheter-based renal nerve ablation and its chronic evolution in a large animal model. J Adv Ther Med Innov Sci. 2016;1:30-38.
25. Sakaoka A, Terao H, Nakamura S, et al. Accurate depth of radiofrequency-induced lesions in renal sympathetic denervation based on a fine histological sectioning approach in a porcine model. Circ Cardiovasc Interv. 2018;11(2):e005779.
26. Rousselle SD, Brants IK, Sakaoka A, et al. Neuromatous regeneration as a nerve response after catheter-based renal denervation therapy in a large animal model: immunohistochemical study. Circ Cardiovasc Interv. 2015;8(5):e002293.
27. Rouselle SD, Dillon KN, Rousselle-Sabiac TH, Brady DA, Tunev S, Tellez A. Historical incidence of spontaneous lesions in kidneys from naive swine utilized in interventional renal denervation studies. J Cardiovasc Transl Res. 2016;9(4):360-367.
28. Rippy MK, Zarins D, Barman NC, Wu A, Duncan KL, Zarins CK. Catheter-based renal sympathetic denervation: chronic preclinical evidence for renal artery safety. Clin Res Cardiol. 2011;100(12):1095-1101.
29. Persu A, Sapoval M, Azizi M, et al. Renal artery stenosis following renal denervation: a matter of concern. J Hypertens. 2014;32(10):2101-2105.
30. Diego-Nieto A, Cruz-Gonzalez I, Martin-Moreiras J, Rama-Merchan JC, Rodriguez-Collado J, Sanchez-Fernandez PL. Severe renal artery stenosis after renal sympathetic denervation. JACC Cardiovasc Interv. 2015;8(11):e193-e194.
31. Bhamra-Ariza P, Rao S, Muller DW. Renal artery stenosis following renal percutaneous denervation. Catheter Cardiovasc Interv. 2014;84(7):1180-1183.
32. Bakris GL, Townsend RR, Flack JM, et al. 12-month blood pressure results of catheter-based renal artery denervation for resistant

hypertension: the SYMPLICITY HTN-3 trial. J Am Coll Cardiol. 2015; 65(13):1314-1321.
33. Patel HC, Dhillon PS, Mahfoud F, et al. The biophysics of renal sympathetic denervation using radiofrequency energy. Clin Res Cardiol. 2014;103(5):337-344.
34. Avitall B, Mughal K, Hare J, Helms R, Krum D. The effects of electrode-tissue contact on radiofrequency lesion generation. Pacing Clin Electrophysiol. 1997;20(12 Pt 1):2899-2910.
35. Zheng X, Walcott GP, Hall JA, et al. Electrode impedance: an indicator of electrode-tissue contact and lesion dimensions during linear ablation. J Interv Card Electrophysiol. 2000;4(4):645-654.
36. Heuser RR, Mhatre AU, Buelna TJ, Berci WL, Hubbard BS. A novel non-vascular system to treat resistant hypertension. EuroIntervention. 2013;9(1):135-139.
37. Booth LC, Nishi EE, Yao ST, et al. Reinnervation of renal afferent and efferent nerves at 5.5 and 11 months after catheter-based radiofrequency renal denervation in sheep. Hypertension. 2015;65: 393-400.
38. Esler MD, Bohm M, Sievert H, et al. Catheter-based renal denervation for treatment of patients with treatment-resistant hypertension: 36 month results from the SYMPLICITY HTN-2 randomized clinical trial. Eur Heart J. 2014;35(26):1752-1759.
39. Sakaoka A, Koshimizu M, Nakamura S, Matsumura K. Quantitative angiographic anatomy of the renal arteries and adjacent aorta in the swine for preclinical studies of intravascular catheterization devices. Exp Anim. 2018;67(2):291-299.
40. Sakakura K, Roth A, Ladich E, et al. Controlled circumferential renal sympathetic denervation with preservation of the renal arterial wall using intraluminal ultrasound: a next-generation approach for treating sympathetic overactivity. EuroIntervention. 2015;10(10):1230-1238.
41. Azizi M, Schmieder RE, Mahfoud F, et al. Endovascular ultrasound renal denervation to treat hypertension (RADIANCE-HTN SOLO): a multicentre, international, single-blind, randomised, sham-controlled trial. Lancet. 2018;391(10137):2335-2345.
42. Fischell TA, Ebner A, Gallo S, et al. Transcatheter alcohol-mediated perivascular renal denervation with the Peregrine system: First-in-human experience. JACC Cardiovasc Interv. 2016;9(6):589-598.

How to cite this article: Sakaoka A, Rousselle SD, Hagiwara H, Tellez A, Hubbard B, Sakakura K. Safety of catheter-based radiofrequency renal denervation on branch renal arteries in a porcine model. *Catheter Cardiovasc Interv*. 2019;93:494–502. https://doi.org/10.1002/ccd.27953